Advanced high-pressure plasma diagnostics with hairpin resonator probe surrounded by film and sheath*

Xu Jin-Zhou(徐金洲)[a)†], Shi Jian-Jun(石建军)[a)], Zhang Jing(张 菁)[a)],
Zhang Qi(张 琪)[b)], Nakamura Keji(中村圭二)[b)], and Sugai Hideo(菅井秀郎)[b)]

[a)] *Department of Applied Physics, College of Science, Donghua University, Shanghai* 201620, *China*
[b)] *Department of Electrical Engineering, School of Engineering, Chubu University* 1200 *Matsumoto-cho, Kasugai, Aichi* 487-8501, *Japan*

(Received 19 August 2009; revised manuscript received 28 December 2009)

The hairpin probe using microwave resonance in plasma is applicable to high pressure 1.33×10^3–1.01×10^5 Pa)) as developed recently. In this work, an analytic model of the hairpin resonator probe surrounded by a thin dielectric layer and a sheath layer is proposed. The correction factor due to these surroundings is analytically found and confirmed by electromagnetic field finite difference time domain simulation, thus enabling the accurate measurement of electron density in a high-pressure non-equilibrium uniform discharge.

Keywords: hairpin resonator probe, simulation, high-pressure plasma, transmission line model
PACC: 5270, 5270D, 5270G

1. Introduction

Since being introduced first by Stenzel in the 1970s, the hairpin or microwave resonator probe has nowadays become a welcome diagnostic technique for low-pressure plasmas.[1−5] This technique is extended to higher pressure ($> 1.33\times10^2$ Pa)) plasma diagnosis with a collision and sheath correction by Sands.[6] However, this corrected model is still not satisfactory when pressure is higher than 1.33×10^3 Pa. Recently, a diagnostic method, i.e. resistive resonant method based on an electromagnetic field finite difference time domain (FDTD) simulation was preliminarily developed.[7] It proposes a possible way for the hairpin resonator probe to be applied to a high-pressure non-equilibrium plasma.

The principle of the hairpin resonator probe is based physically on the dependence of measured reflection spectrum in terms of the full width of half maximum (FWHM), resonant frequency $f_{\rm r}$ and reflection coefficient $\Gamma_{\rm min}$ on propagation constant (γ) of probe wires or transmission lines ($\gamma=\alpha+{\rm j}\beta$, α and β are the attenuation constant and the phase constant, respectively). On the other hand, the propagation constant (γ) is correlated to the distributed elements of the probe wires, i.e. inductance (L), capacitance (C), resistance (R) of line and leakage conductance (G). Furthermore, the distributed elements are influenced by plasma characteristic.

By inserting the probe into plasma, the metal surface of the probe will be bombarded by energetic ions and oxidised by chemical active species. The photoelectrons will also be emitted from probe surface by ultraviolet radiation. In practical applications, the probe surface is normally protected by a thin dielectric layer to reduce these effects of surface sputtering, contamination and photo-electron emission.

In this work, an analytical model of hairpin resonator probe coated with a thin dielectric protection layer and wrapped by a sheath layer is proposed. A corrected diagnostic method is then developed and studied for diagnosing high pressure non-equilibrium plasma by electromagnetic field simulation.

*Project supported by the National Natural Science Foundation of China (Grant No. 10835004), and the 2nd Knowledge Cluster Research Project of Japan: Tokai Region Nanotechnology Manufacturing Cluster (Innovation of Environment Friendly Highly Functional Materials and Devices).
†Corresponding author. E-mail: jzxu@dhu.edu.cn
© 2010 Chinese Physical Society and IOP Publishing Ltd

2. Analytic model of hairpin resonator probe protected by thin dielectric film and sheath layer

2.1. Simulation method of hairpin resonator probe

The hairpin resonator probe (without protection film) can also be used to diagnose the high pressure non-equilibrium plasma in principle. The electron density can be obtained from the following relation between normalised width of reflection spectrum $(\Delta f/f_{\rm r})$ and plasma characteristics $(\sigma_{\rm p}, \varepsilon_{\rm pr})$:[7]

$$\frac{1}{l}\left[\ln\left(\frac{\pi\times\Delta f}{2f_{\rm r}}+1\right)-\ln\left(\frac{\pi\times\Delta f_{\rm vac}}{2f_{\rm vac}}+1\right)\right] = \frac{120\pi\sigma_{\rm p}}{\sqrt{\varepsilon_{\rm pr}}}, \quad (1)$$

$$\sigma_{\rm p} = \frac{\varepsilon_0\omega_{\rm pe}^2\nu_{\rm m}}{\omega^2+\nu_{\rm m}^2},$$

$$\varepsilon_{\rm pr} = 1-\frac{\omega_{\rm pe}^2}{\omega^2+\nu_{\rm m}^2}, \quad (2)$$

where $\omega = 2\pi f$, $\varepsilon_{\rm pr}$ and $\sigma_{\rm p}$ are the real parts of plasma permittivity and plasma conductivity, respectively. $f_{\rm vac}$ and $\Delta f_{\rm vac}$ are the resonant frequency and the FWHM of the reflection spectra in vacuum or in the absence of plasma.

The electromagnetic field FDTD simulation is a convenient tool for studying the problems concerned with electromagnetic phenomena in plasmas.[8] In the present work, one of commercially available softwares, CST MICROWAVE STUDIO,[9] is used to simulate the microwave signal transmitted in and reflected from the probe. The simulation is carried out by determining the characteristics of microwave power source connected to probe, i.e. port type, impedance, location and excitation signal in the software. The plasma is considered to be a cold plasma medium, which is described by gas pressure, plasma density and electron temperature through the Drude dispersion formula $\varepsilon_{\rm pr}(\omega) = 1-\omega_{\rm p}^2/\omega(\omega-{\rm j}\nu_{\rm m})$. The probe essentially acts as a half-wavelength dipole antenna, and the resonance occurs at a particular frequency of $f_{\rm r}$ by sweeping microwave source frequency f in an appropriate range. The diagram of hairpin resonator probe is shown in Fig. 1. In the case, a small microwave power fed at position $z=-l$ is reflected from the open end position $z=0$, and the power reflection spectrum is displayed as s-parameter s_{11} or reflection coefficient $\Gamma(f)$ through $|\Gamma| = |(Z_{\rm in}-Z_{0\rm s})/(Z_{\rm in}+Z_{0\rm s})|$ $(Z_{0\rm s}=50\ \Omega)$.[9,10]

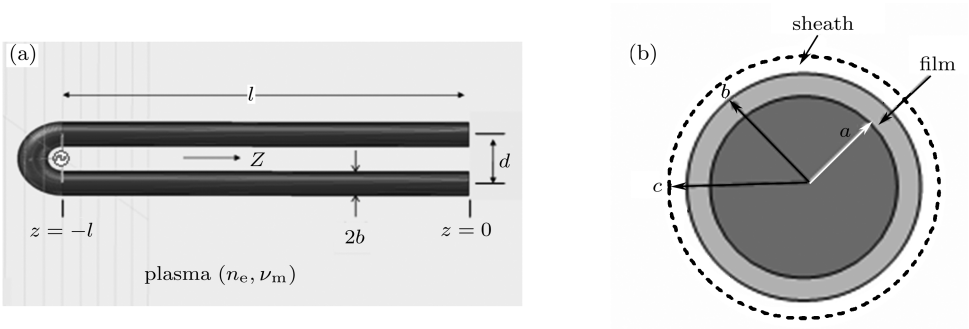


Fig. 1. Model of hairpin resonator probe with a thin dielectric film (a), and radial cross section of a probe metal wire covered with a film and a sheath separately (b).

2.2. Model of probe with protection film and sheath layer

Hairpin resonator probe is well considered as parallel-wire transmission lines terminated with an open-circuited end.[7] When the surface of hairpin resonator probe is coated by a thin dielectric film with relative permittivity of $\varepsilon_{\rm die}$ and is assumed to be immersed into a uniform (in region with the scale of probe) argon plasma with electron density of $n_{\rm e}$ and temperature of $T_{\rm e}$ (eV) at pressure of p (Pa), an analytical model of the probe with a protection film and a sheath layer can be derived from a lumped equivalent circuit for infinitesimal section of transmission line as shown in Fig. 2. Here, the probe radius of metal wire is a, the film thickness $h(b=a+h)$, and the thickness of sheath $d_{\rm s}$ with outermost radius $c=b+d_{\rm s}$). The sheath is regarded as a vacuum layer. $C_{\rm d,s}$ is the capacitance in series with a sheath layer and a dielectric film, which are given by $C_{\rm s} = 2\pi\varepsilon_0/\ln(c/b)$ and $C_{\rm d} = 2\pi\varepsilon_0\varepsilon_{\rm die}/\ln(b/a)$, respectively.

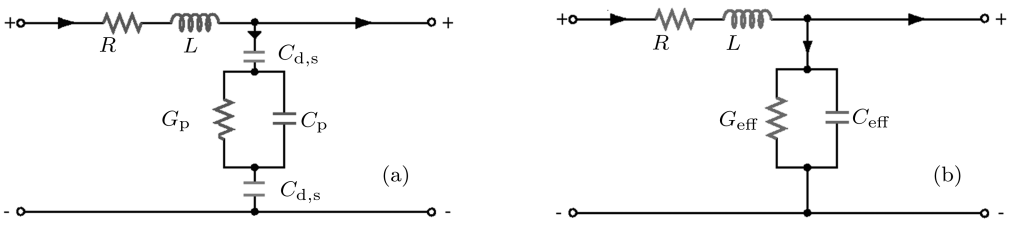


Fig. 2. Transmission line model of hairpin probe wires when wrapped by protection film and sheath layer, where panel (a) shows lumped-element circuit model of probe with protection film and sheath layer, and panel (b) displays effective $G_{\rm eff}$ and $C_{\rm eff}$.

Letting the voltage across the plasma be $v_{\rm p}$ and the voltage across the film and the sheath be $v_{\rm d,s}$ in Fig. 2(a), the current in the unit length of transmission line is written as[11]

$$\begin{aligned} &i' = i_{\rm p} + C_{\rm p}\frac{{\rm d}v_{\rm p}}{{\rm d}t} = C_{\rm d,s}\frac{{\rm d}v_{\rm d,s}}{{\rm d}t},\\ &v = v_{\rm p} + v_{\rm d,s},\\ &i_{\rm p} + C_{\rm p}\frac{{\rm d}v}{{\rm d}t} = (C_{\rm d,s}+C_{\rm p})\frac{{\rm d}v_{\rm d,s}}{{\rm d}t} = \frac{C_{\rm d,s}+C_{\rm p}}{C_{\rm d,s}}i',\\ &i' = \frac{i_{\rm p} + \dfrac{C_{\rm p}v}{\partial t}}{1+\dfrac{C_{\rm p}}{C_{\rm d,s}}} = \frac{G_{\rm p}v_{\rm p} + \dfrac{C_{\rm p}\partial v}{\partial t}}{1+\dfrac{C_{\rm p}}{C_{\rm d,s}}}, \end{aligned} \tag{3}$$

where $C_{\rm d,s} = C_{\rm d}C_{\rm s}/(C_{\rm d}+C_{\rm s})$, and the conduction current through plasma $i_{\rm p} = G_{\rm p}v_{\rm p}$. The current of i' is equivalent to $-\partial i(z,t)/\partial z$ in transmission line equation of time domain.[10] If the driven voltage is time harmonic, Eq. (3) is then written in phasor form as

$$\tilde{I}' = \frac{G_{\rm p}\tilde{V}_{\rm p} + {\rm j}\omega C_{\rm p}\tilde{V}}{1+\dfrac{C_{\rm p}}{C_{\rm d,s}}}. \tag{4}$$

In the microwave frequency range, with thin dielectric film and thin sheath layer, the approximation of $\tilde{V}_{\rm d,s} = \tilde{I}'/{\rm j}\omega C_{\rm d,s} \propto \tilde{I}'(h/a + \varepsilon_{\rm die}d_{\rm s}/a)/{\rm j}\omega \approx 0$. can be made. It suggests that the voltage mostly drops across the plasma and $\tilde{I}_{\rm p} = G_{\rm p}\tilde{V}_{\rm p} \approx G_{\rm p}\tilde{V}$. Then

$$\tilde{I}' \cong \frac{G_{\rm p}+{\rm j}\omega C_{\rm p}}{1+\dfrac{C_{\rm p}}{C_{\rm d,s}}}\tilde{V} = (G_{\rm eff}+{\rm j}\omega C_{\rm eff})\tilde{V}. \tag{5}$$

Thus the equivalent lumped-element circuit with effective capacitance ($C_{\rm eff}$) and conductance ($G_{\rm eff}$) is shown in Fig. 2(b), and correspondingly $C_{\rm eff}$ and $G_{\rm eff}$ are given respectively as

$$\begin{aligned} C_{\rm eff} &= \frac{C_{\rm p}}{1+\dfrac{C_{\rm p}}{C_{\rm d,s}}} = \frac{\pi\varepsilon_0\varepsilon_{\rm pr(eff)}}{\ln\left[\dfrac{d}{2a}+\sqrt{\left(\dfrac{d}{2a}\right)^2-1}\right]},\\ G_{\rm eff} &= \frac{G_{\rm p}}{1+\dfrac{C_{\rm p}}{C_{\rm d,s}}} = \frac{\pi\sigma_{\rm p(eff)}}{\ln\left[\dfrac{d}{2a}+\sqrt{\left(\dfrac{d}{2a}\right)^2-1}\right]}, \end{aligned} \tag{6}$$

where the effective permittivity and the effective conductivity of plasma, respectively, are

$$\begin{aligned} \varepsilon_{\rm pr(eff)} &= \frac{\varepsilon_{\rm pr}}{\Lambda},\\ \sigma_{\rm p(eff)} &= \frac{\sigma_{\rm p}}{\Lambda}, \end{aligned} \tag{7}$$

where Λ is the correction factor induced by the film and the sheath layer and derived from Eq. (6) to be

$$\Lambda = \frac{\ln\left[\dfrac{d}{2c}+\sqrt{\left(\dfrac{d}{2c}\right)^2-1}\right] + \dfrac{\varepsilon_{\rm pr}}{\varepsilon_{\rm die}}\left[\ln\left(\dfrac{b}{a}\right)+\varepsilon_{\rm die}\ln\left(\dfrac{c}{b}\right)\right]}{\ln\left[\dfrac{d}{2a}+\sqrt{\left(\dfrac{d}{2a}\right)^2-1}\right]}. \tag{8}$$

3. Corrected method of high-pressure plasma diagnostics

From the model of hairpin resonator probe described in Section 2, the attenuation constant of the probe wires can be written as

$$
\begin{aligned}
\alpha &= \frac{1}{2}\left\{R\sqrt{\frac{C_{\rm eff}}{L}}+G_{\rm eff}\sqrt{\frac{L}{C_{\rm eff}}}\right\}\\
&= \frac{1}{2}\left\{R_{\rm rad}\frac{\sqrt{\varepsilon_{\rm pr(eff)}}}{120\ln\left[\dfrac{d}{2a}+\sqrt{\left(\dfrac{d}{2a}\right)^2-1}\right]}+\frac{\sqrt{f_{\rm r}\mu_0\varepsilon_{\rm pr(eff)}/\pi\sigma_{\rm line}}}{240a\ln\left[\dfrac{d}{2a}+\sqrt{\left(\dfrac{d}{2a}\right)^2-1}\right]}+\frac{120\pi\sigma_{\rm p(eff)}}{\sqrt{\varepsilon_{\rm pr(eff)}}}\right\}\\
&= \frac{1}{2\Lambda^{1/2}}\left\{R_{\rm rad}\frac{\sqrt{\varepsilon_{\rm pr}}}{120\ln\left[\dfrac{d}{2a}+\sqrt{\left(\dfrac{d}{2a}\right)^2-1}\right]}+\frac{\sqrt{f_{\rm r}\mu_0\varepsilon_{\rm pr}/\pi\sigma_{\rm line}}}{240a\ln\left[\dfrac{d}{2a}+\sqrt{\left(\dfrac{d}{2a}\right)^2-1}\right]}+\frac{120\pi\sigma_{\rm p}}{\sqrt{\varepsilon_{\rm pr}}}\right\}\\
&\cong \frac{1}{2\Lambda^{1/2}}\left\{R_{\rm rad}\frac{\sqrt{\varepsilon_{\rm pr}}}{120\ln\left[\dfrac{d}{2a}+\sqrt{\left(\dfrac{d}{2a}\right)^2-1}\right]}+\frac{120\pi\sigma_{\rm p}}{\sqrt{\varepsilon_{\rm pr}}}\right\},
\end{aligned}
\tag{9}
$$

where R is the sum of radiation resistance and self-loss resistance of probe.[12] As the probe wires are assumed to be made of metal with perfect conductivity, the loss of probe itself is neglected in formula (9). $R_{\rm rad}$ is the averaged radiation resistance of probe wires in unit length, which has the same magnitudes in vacuum and plasma. Following the same procedure as that in Ref. [7], the relationship between the normalised width $(\Delta f/f_{\rm r})$ and plasma characteristics ($\sigma_{\rm p}$, $\varepsilon_{\rm pr}$) in Eq. (1) is rewritten as

$$
\frac{1}{l}\Lambda_{\rm vac}^{1/2}\left[\left(\frac{\Lambda_{\rm p}}{\Lambda_{\rm vac}}\right)^{1/2}\ln\left(\frac{\pi\times\Delta f_{\rm p}}{2f_{\rm r}}+1\right)-\sqrt{\varepsilon_{\rm pr}}\ln\left(\frac{\pi\times\Delta f_{\rm vac}}{2f_{\rm vac}}+1\right)\right]=\frac{120\pi\sigma_{\rm p}}{\sqrt{\varepsilon_{\rm pr}}},
\tag{10}
$$

where $\Lambda_{\rm p}$ and $\Lambda_{\rm vac}$ are the corrected factors as shown by Eq. (8), in plasma and vacuum, respectively.

Equation (8) indicates that the value of Λ is influenced by both geometrics factors such as radius (a), axis pitch of probe wires (d), dielectric film thickness (h), sheath layer thickness ($d_{\rm s}$), and electrical parameters such as plasma permittivity ($\varepsilon_{\rm pr}$), and dielectric film permittivity ($\varepsilon_{\rm die}$). In practical applications, the characteristics of the protection film should be chosen such that the requirements of less sputtering, less surface contamination and less electron emission in a plasma medium are satisfied.

In general, the protection film thickness (h) is on the order of several micrometers and sheath thickness ($d_{\rm s}$) is about a few tens of micrometers, which are both much smaller than the radius of probe wire and the wire width. Taking $c/a = 1 + h/a + d_{\rm s}/a$, $b/a = 1 + h/a$, and $c/b \approx 1 + d_{\rm s}/a$, the correction factor described by Eq. (8) is then simplified into

$$
\Lambda \approx 1 - mh/a - nd_{\rm s}/a,
\tag{11}
$$

where

$$
m = \frac{1}{\ln\left[\dfrac{d}{2a}+\sqrt{\left(\dfrac{d}{2a}\right)^2-1)}\right]}\left(\frac{d/2a}{\sqrt{(d/2a)^2-1}}-\frac{\varepsilon_{\rm pr}}{\varepsilon_{\rm die}}\right),
$$

$$
n = \frac{1}{\ln\left[\dfrac{d}{2a}+\sqrt{\left(\dfrac{d}{2a}\right)^2-1)}\right]}\left(\frac{d/2a}{\sqrt{(d/2a)^2-1}}-\varepsilon_{\rm pr}\right).
$$

The influence of geometric dimension of probe on sheath correction can be deduced from Eq. (11). When the radius of probe wire is relatively large (on the order of millimeters), the value of $d_{\rm s}/a$ is very small. Additionally a larger probe radius also leads to the reduction in the value n especially in high-pressure plasmas as the width of probe (d) should satisfy the condition $d \geq 2(d_{\rm s}+b)$. In this case, as known from Eq. (11), the sheath influence is further depressed. However, the increase of the probe width is consequentially at the expense of increasing the perturbation to plasma, reducing the spatial resolution and the resonant quality. These are in accordance with the results discussed in Refs. [2] and [6]. A proposed solution for these problems is to optimize the dimensions of probe with a comprehensive consideration of width and radius, which reduces the magnitude of the term $(nd_{\rm s}/a)$ to be as small as possible or even negligible.

At high pressures ($\nu_{\rm m}^2 \gg \omega_{\rm pe}^2, \omega^2$), plasma permittivity $\varepsilon_{\rm pr}$ is close to unity and plasma conductivity $\sigma_{\rm p}$ is $\sim \varepsilon_0\omega_{\rm pe}^2/\nu_{\rm m}$. Substituting these values into Eq. (10) yields Eq. (12) at $\Delta f/f_{\rm r} < 1$ as follows:

$$\left(\frac{\Delta f}{f_{\rm r}}\right)_{\rm c} = \left(\frac{\Lambda_{\rm p}}{\Lambda_{\rm vac}}\right)^{1/2}\left(\frac{\Delta f}{f_{\rm r}}\right)_{\rm p} - \left(\frac{\Delta f}{f_{\rm r}}\right)_{\rm vac} = \frac{1}{\Lambda_{\rm vac}^{1/2}}\frac{240l\varepsilon_0\omega_{\rm pe}^2}{\nu_{\rm m}}. \tag{12}$$

So, the density of high-pressure plasma can be estimated by the corrected method of hairpin resonator probe to be

$$n_{\rm e} = 1.48\times10^{17}\Lambda_{\rm vac}^{1/2}\frac{\nu_{\rm m}}{l}\left(\frac{\Delta f}{f_{\rm r}}\right)_{\rm c}, \tag{13}$$

where $n_{\rm e}$ is in $\rm m^{-3}$, $\nu_{\rm m}$ is in GHz, and l is in mm. Electron-molecule elastic collision frequency $\nu_{\rm m}$ depends on electron temperature $T_{\rm e}$ and pressure through $\nu_{\rm m} = K(T_{\rm e})p/k_{\rm B}T_{\rm m}$. The data base for the collision rate constant is available in the literature for typical gas such as He, Ar, O_2, etc.

In the double hairpin probe technique proposed in the previous study,[7] the same sheath layer surrounds the probe wires immersed in the same plasmas. From formulas (11) and (12), the sheath thickness($d_{\rm s}$) and the correction factor ($\Lambda_{\rm p}$) can be determined by double hairpin probe with different geometrics and / or dielectric film, described by

$$d_{\rm s} = \frac{(2-m_1h_1/a_1)\dfrac{1}{l_1}\left[\left(\dfrac{\Delta f}{f_{\rm r}}\right)_{\rm p,1} - \left(\dfrac{\Delta f}{f}\right)_{\rm vac,1}\right] - (2-m_2h_2/a_2)\dfrac{1}{l_2}\left[\left(\dfrac{\Delta f}{f_{\rm r}}\right)_{\rm p,2} - \left(\dfrac{\Delta f}{f}\right)_{\rm vac,2}\right]}{\dfrac{n_1}{l_1a_1}\left(\dfrac{\Delta f}{f_{\rm r}}\right)_{\rm p,1} - \dfrac{n_2}{l_2a_2}\left(\dfrac{\Delta f}{f_{\rm r}}\right)_{\rm p,2}}. \tag{14}$$

Here, the subscripts of 1, 2 denote the probe numbers. The quantities of m and n are the factors corresponding to the probe geometrical scale and the permittivity of thin dielectric film, as indicated in formula (1).

4. FDTD simulation study of corrected method

For hairpin probe with geometric parameters of a, d and l being 1, 4 and 27 mm respectively and silicon dioxide (SiO_2) film selected as a probe protection film, the curves for variations of Λ with film thickness in given plasmas are shown in Fig. 3, those for the case of no sheath correction are also displayed for comparison. The influence of film thickness is almost linear when pressure is larger than 4.80×10^4 Pa. This can be also confirmed by $\Lambda = \Lambda_{\rm p} \approx 1-0.676h/a-0.117d_{\rm s}/a$ as derived from formula (11) when $\varepsilon_{\rm pr}/\varepsilon_{\rm die} < 1$ and $\varepsilon_{\rm pr} \approx 1$. However, if the pressure is lower than 4.80×10^4 Pa, the variation turns nonlinear for lower electron temperatures. This is caused mainly by the collision frequency $\nu_{\rm m}$ dependence of $\varepsilon_{\rm pr}$ as displayed in Fig. 4.

For the described probe size, the deviation of Λ from 1, induced by the protection SiO_2 film, is less than 0.7% when its thickness is no more than 10 μm. This can be confirmed by $\Lambda_{\rm vac} \approx 1-0.676h/a$ from formula (11) and Fig. 3. Furthermore, the deviation from $\Lambda_{\rm vac}$, caused by plasma sheath, is less than 2% for the plasmas with electron densities ranging from 1–10×10^{16} $\rm m^{-3}$ at $T_{\rm e} < 1.0$ eV. It suggests that the estimated density from formula (12) or (13) would re-

sult in only about 1% increase if the sheath correction is neglected.

When the present probe is coated by a SiO_2 layer of thickness 2.0 μm (corrected factor $\Lambda_{\rm vac} = 0.99865$), and then inserted into a plasma with $n_{\rm e} = 4\times10^{16}$ m^{-3}, $T_{\rm e} = 1.0$ eV at $p = 2.13\times10^4$ Pa, the typical spatial distribution of current density around the probe and corresponding reflection spectrum obtained by FDTD are presented in Fig. 5. Table 1 presents the characteristics of reflection spectra, i.e. dependences of $f_{\rm r}$ and FWHM on frequency, in some plasmas.

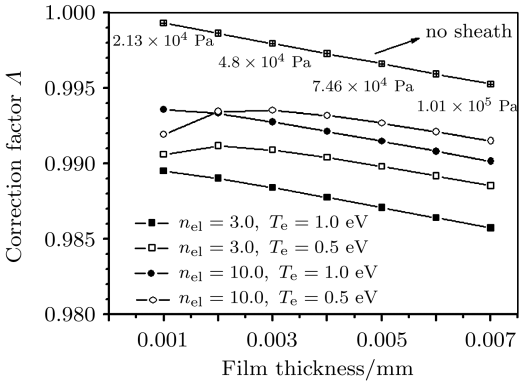


Fig. 3. Effects of plasma parameters and film thickness on correction factor, where $d_{\rm s}$ is taken to be $\pi^{1/2}\lambda_{\rm De}$,[13] $n_{\rm el}$ is in 10^{16} m^{-3}.

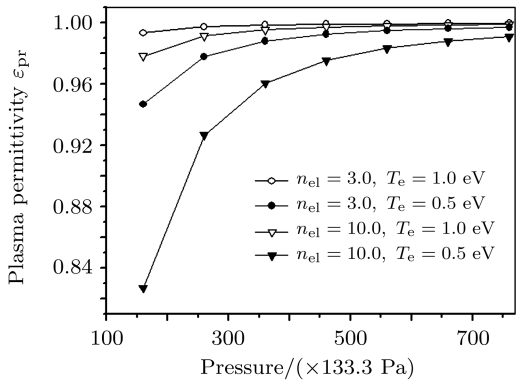


Fig. 4. Dependences of plasma permittivity on pressure at resonant frequency in plasmas with different densities and temperatures.

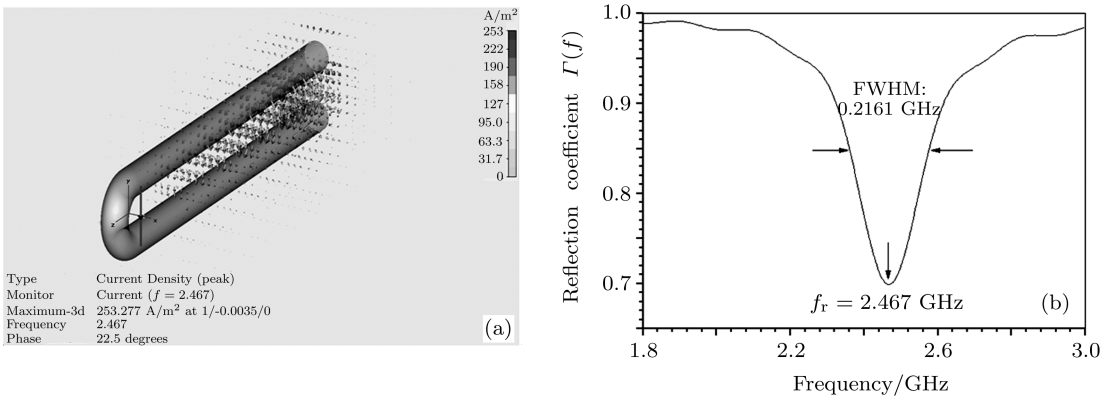


Fig. 5. FDTD simulation results, where panel (a) shows current distribution around the probe and panel (b) displays corresponding reflection spectrum (b).

Table 1. Characteristics of reflection spectra.

P/Pa		2.13×10^4		1.01×10^5
$T_{\rm e}$/eV		0.5	1.0	0.5
$n_{\rm e}/10^{16}{\rm m}^{-3}$	2	*2.5030(0.2855)	2.4610(0.1260)	2.4580(0.0928)
	4	2.5510(0.5476)	2.4670(0.2161)	2.4610(0.1529)
	6	2.6020(0.8079)	2.4730(0.3122)	2.4640(0.2131)
	8	2.6650(1.0744)	2.4790(0.4075)	2.4640(0.2674)
	10	2.7190(1.2217)	2.4850(0.4894)	2.4670(0.3317)

* Resonant frequency (GHz) and FWHM (GHz) are bracketed separately.

By taking the electron collision frequency in the form of $\nu_{\rm m} \approx 5.64 \times 10^6 \times 133.3\ pT_{\rm e}^{1.609}({\rm s}^{-1})$,[13] the electron density of plasmas estimated from formula (13) is shown in Fig. 6. It shows the electron densities determined by the corrected method are very close at different pressures and temperatures. The larger deviation in a high density plasma, especially at 2.13×10^4 Pa and $T_{\rm e} = 0.5$ eV, is caused mainly by assuming $\varepsilon_{\rm pr} \sim 1$ in Eq. (11), which has been analysed in Fig. 4.

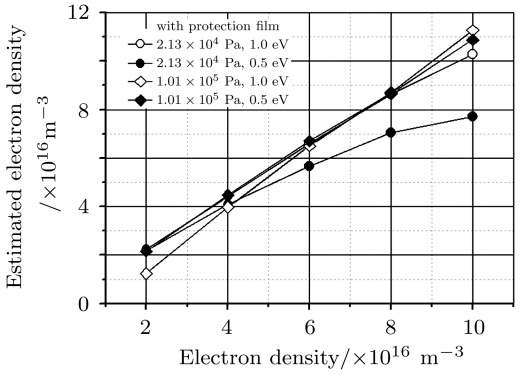


Fig. 6. The estimated election density using the corrected method.

5. Conclusion

An analytic model of the transmission line for the hairpin resonator probe with a dielectric film and a sheath layer is developed. The corrected method of electron density measurement and the influence of probe geometrical and plasma parameters are also studied by using electromagnetic field simulation. Compared with the protection film, the sheath layer has a significant effect on the correction factor Λ. The double-probe method of electron density measurement can be used to determine the sheath width. However, by appropriately selecting the dimensions of probe width and probe radius, the sheath influence can be reduced or even neglected in high-pressure plasmas. For the hairpin probe with geometric parameters of a and d being 1 and 4 mm respectively, it is indicated that the value of Λ induced by the protection film would be less than 0.7% if SiO_2 film thickness is no more than 10 μm, while the deviation caused by the sheath is less than 2% for plasma density in a range from 1–10$\times 10^{16}$ m^{-3} at $T_{\rm e} < 1.0$ eV. The results estimated from the electromagnetic field FDTD simulation suggest that the developed corrected method can be applied to measuring the electron density at a high-pressure.

References

[1] Stenzel R L 1976 *Rev. Sci. Instrum.* **47** 603

[2] Piejak P B, Godyak V A, Garner P, Alexandrovich B M and Sternberg N 2004 *J. Appl. Phys.* **95** 3785

[3] Karkari S K and Elilingbore A R 2006 *Appl. Phys. Lett.* **88** 101501

[4] Milosavljevic V, Karkari S K and Elilingbore A R 2007 *Plasma Sources Sci. Technol.* **16** 304

[5] Karkari S K, Doggett B, Gaman C, Donnelly T, O'Farrel D, Ellingboe A R and Lunney J G 2008 *Plasma Sources Sci. Technol.* **17** 032001

[6] Sands B L, Siefert N S and Ganguly B N 2007 *Plasma Sources Sci. Technol.* **16** 716

[7] Xu J Z, Nakamura K, Zhang Q and Sugai H 2009 *Plasma Sources Sci. Technol.* **18** 045009

[8] Chen Z Q, Liu M H, Lan C H, Chen W, Tang L, Luo Z Q, Yan B R, Lü J H and Hu X W 2009 *Chin. Phys.* B **18** 3484

[9] CST Microwave Studio 2008 *WWW.CST.COM*

[10] Inan U S and Inan A S 1999 *Engineering Eletromagnetics* (Canifornia: Addision Wesley Longman) p156

[11] Merbahi N, Sewraj N, Marchal F and Ledru G 2004 *10th International Symposium on the Science & Technology of Light Source*, Toulouse, 18–22 July, 2004 p276

[12] Ulaby F T 2007 *Fundamentals of Applied Electromagnetics* (translatd by Yin H J) (Beijing: Post & Telecom Press) p349 (in Chinese)

[13] Lieberman M A and Lichtenbeg A J 2005 *Principles of Plasma Discharges and Materials Processing* 2nd edition (New Jersey: Wiley) p81